ELSEVIER

Contents lists available at ScienceDirect

Measurement

journal homepage: www.elsevier.com/locate/measurement





Least squares approach to standard platinum resistance thermometer subrange inconsistency reduction with redundant gallium and indium fixed points

Vincencij Žužek^{a,*}, Richard Rusby^b, Jonathan Pearce^b, Andrea Peruzzi^c, Jovan Bojkovski^a

- ^a University of Ljubljana, Slovenia
- ^b National Physical Laboratory, UK
- c National Research Council of Canada, Canada

ARTICLE INFO

Keywords:

Standard platinum resistance thermometer (SPRT)

Subrange inconsistency (SRI)

Non-uniqueness

International Temperature Scale of 1990 (ITS-

Polynomial least squares

Propagation of uncertainty (PoU)

ABSTRACT

The International Temperature Scale of 1990 (ITS-90) defines several different and sometimes overlapping temperature subranges. Where overlap occurs, different definitions of the temperature t_{90} exist that have equal status but produce different results. This discrepancy is called type 1 non-uniqueness or subrange inconsistency (SRI)

In this paper, the SRI of the water-aluminum/water-zinc (SRI(Al:Zn)) and of the water-zinc/water-tin (SRI(Zn:Sn)) subranges of the ITS-90 were investigated for three cases. In the first case, the calculations followed the ITS-90 prescribed procedure. In the second case, the SPRT was calibrated at all fixed points of the subrange and its deviation function was then determined using the least squares method. In the third case, the least squares method was weighted by the uncertainties at each of the fixed points. One benefit of the least squares approach over exact interpolation is the reduction in uncertainty propagated from the fixed points. The calculations were applied to a large ensemble of 30 different SPRTs from the database of the Laboratory of Metrology and Quality at the University of Ljubljana, Slovenia. The sample consisted mainly of SPRTs manufactured by Fluke, Rosemount and AccuMac.

The difference in the mean and standard deviation of SRI(Al:Zn) for the three cases was small, amounting to less than 0.06 mK. On the other hand, the mean of SRI(Zn:Sn) decreased from 0.73 mK to 0.01 mK and the standard deviation decreased from 1.25 mK to 0.43 mK when the weighted least squares approach was applied. Furthermore, the total propagated uncertainty from the fixed points decreased in particular temperature ranges with weighted least squares, especially from 50 °C to 300 °C (by about 50% compared to the ITS-90 case) and to a lesser extent from 400 °C to 600 °C (by about 10% compared to the ITS-90 case). The contribution of the difference in the uncertainty propagation between pairs of subranges to SRI was estimated to be at least 50% in all cases. According to the presented results, it can be advantageous to calibrate the SPRT at all available fixed points in the selected temperature subrange and then determine its deviation function using the weighted least squares method.

1. Introduction

The International Temperature Scale of 1990 (ITS-90) [1] defines the temperature t_{90} that is a close approximation to the equivalent thermodynamic temperature t which is in turn one of the seven base quantities in the International System of Units (SI) [2]. Measurements of t_{90} are more practical, repeatable and precise in comparison with measurements of t and are one of the most frequently made among the

physical quantities.

Standard platinum resistance thermometers (SPRTs) are used to realize t_{90} in the temperature range between the triple point of equilibrium hydrogen at $-259.3467\,^{\circ}\text{C}$ and the freezing point of silver at 961.78 °C, together with specified defining temperature fixed points and interpolation procedures [1]. The fixed points are triple, melting and freezing points of pure substances with defined temperature values. In this work we investigated only long-stem SPRTs in the range between

E-mail address: vincencij.zuzek@fe.uni-lj.si (V. Žužek).

^{*} Corresponding author.

V. Žužek et al. Measurement 220 (2023) 113400

the triple point of water at 0.01 $^{\circ}\text{C}$ and the freezing point of aluminum at 660.323 $^{\circ}\text{C}.$

To calculate t_{90} from the measured electrical resistance R of a SPRT, several steps are needed [3]. Firstly, R is divided by the resistance of the SPRT at the triple point of water (TPW) to yield the resistance ratio W (equation (1)). W is then corrected with the deviation function ΔW of the SPRT to yield the reference resistance ratio W_r (equation (2)).

$$W(t_{90}) = \frac{R(t_{90})}{R(TPW)} \tag{1}$$

$$W_r(t_{90}) = W(t_{90}) - \Delta W(t_{90}) \tag{2}$$

In the temperature range from the triple point of water to the freezing point of aluminum, the ΔW are polynomial functions of W-1 with degrees up to 3. The defined fixed points and values of ratio W_r in this range are given in Table 1. For a particular SPRT, the coefficients of the ΔW polynomial functions are determined from measurements of W at these fixed points. Finally, temperature t_{90} is calculated from W_r , using a polynomial function specified in the ITS-90 [1].

The ITS-90 defines several different and sometimes overlapping temperature subranges. Where overlapping of these subranges occurs, different definitions of t_{90} exist at the same temperature that have equal status but produce different results: for the same R, the two definitions return different t_{90} values. In the original text of the ITS-90, these differences were deemed "of negligible practical importance", but nowadays they are in fact significant in comparison with many stated SPRT measurement and calibration uncertainties. This discrepancy is called type 1 non-uniqueness or subrange inconsistency (SRI) and arises as a combined effect of three contributions [4,5]:

- scale contribution due to non-ideal W_r values of the defining fixed points (same for all SPRTs, see Table 1),
- SPRT contribution due to differences in the SPRT characteristics that lead to differences in the interpolations,
- contribution due to propagation of uncertainty (PoU) from calibration of the SPRT at fixed points in the two subranges.

For example, the most commonly determined is the SRI between the water-zinc and water-aluminum subranges of a particular SPRT, denoted as SRI(Al:Zn) [6–9]. These two subranges, which overlap in the temperature range from the triple point of water to the freezing point of zinc, prescribe two different ΔW functions (quadratic for the water-zinc subrange and cubic for the water-aluminum subrange), hence the calculated temperatures are not fully consistent. The current mean value for SRI(Al:Zn) according to existing literature is between 0.04 mK and 0.23 mK with standard deviation between 0.29 mK and 0.48 mK [4,6].

In this paper the SRI(Al:Zn) and SRI(Zn:Sn) were investigated for three cases. In the first case, the calculations followed the ITS-90 prescribed procedure, as described in [1]. In the second case, the SPRT was calibrated at all fixed points of the water-aluminum subrange (all fixed points from Table 1) and ΔW were determined with the least squares method, still at degree 3 and 2 respectively, taking into account the additional fixed points. In the third case, the least squares method was

Table 1 ITS-90 temperature fixed points in the range between the triple point of water and the freezing point of aluminum. The last column is the expanded uncertainty (k=2) of the Laboratory of Metrology and Quality (LMK) at the University of Liubljana.

fixed point	<i>t</i> ₉₀ / °C	W_{r}	U/mK
triple point of water (H ₂ O)	0.01	1.00000000	0.15
melting point of gallium (Ga)	29.7646	1.11813889	0.4
freezing point of indium (In)	156.5985	1.60980185	0.9
freezing point of tin (Sn)	231.928	1.89279768	1
freezing point of zinc (Zn)	419.527	2.56891730	1.5
freezing point of aluminum (Al)	660.323	3.37600860	2.5

weighted with the LMK uncertainties at each of the fixed points.

One benefit of the least squares approach over exact interpolation is the reduction in uncertainty propagated from the fixed points [10]. It is therefore of interest to determine whether the SRI also decreases. Another possible approach to SRI reduction is to decrease the scale contribution by selecting different fixed points or interpolation functions [11–13].

2. Least squares approach

The cubic deviation function in the water-aluminum subrange has the form (3):

$$\Delta W = a \cdot (W - 1) + b \cdot (W - 1)^2 + c \cdot (W - 1)^3$$
(3)

The ITS-90 specifies that the coefficients a, b and c are calculated from calibrations of the SPRT at the tin, zinc and aluminum freezing points and at the water triple point, to obtain the resistance ratios $W_{\rm Sn}$, $W_{\rm Zn}$ and $W_{\rm Al}$. The exact solution of the system of three linear equations with three unknown quantities is then uniquely determined (equation (4)). In Fig. 1, deviations from reference ratios for a typical SPRT are shown as blue asterisks and the red line is the resulting deviation function. Note that in this and all the ITS-90 interpolation equations, $\Delta W = 0$ at the triple point of water, where W is identically equal to 1.

$$X = A^{-1} \cdot B \tag{4}$$

$$X = \begin{bmatrix} a \\ b \\ c \end{bmatrix} A = \begin{bmatrix} W_{Sn} - 1 & (W_{Sn} - 1)^2 & (W_{Sn} - 1)^3 \\ W_{Zn} - 1 & (W_{Zn} - 1)^2 & (W_{Zn} - 1)^3 \\ W_{Al} - 1 & (W_{Al} - 1)^2 & (W_{Al} - 1)^3 \end{bmatrix} B = \begin{bmatrix} W_{Sn} - W_{Sn,r} \\ W_{Zn} - W_{Zn,r} \\ W_{Al} - W_{Al,r} \end{bmatrix}$$

If we include also the additional measurements at gallium and indium points (W_{Ga} and W_{In}), we get an overdetermined system of 5 linear equations with 3 unknown quantities. The application of the weighted least squares method provides a solution (equation (5) and Fig. 2):

$$X = (A^T \cdot W \cdot A)^{-1} \cdot A^T \cdot W \cdot B \tag{5}$$

$$X = \begin{bmatrix} a \\ b \\ c \end{bmatrix} A = \begin{bmatrix} W_{Ga} - 1 & (W_{Ga} - 1)^2 & (W_{Ga} - 1)^3 \\ W_{In} - 1 & (W_{In} - 1)^2 & (W_{In} - 1)^3 \\ W_{Sn} - 1 & (W_{Sn} - 1)^2 & (W_{Sn} - 1)^3 \\ W_{Zn} - 1 & (W_{Zn} - 1)^2 & (W_{Zn} - 1)^3 \\ W_{Al} - 1 & (W_{Al} - 1)^2 & (W_{Al} - 1)^3 \end{bmatrix} B = \begin{bmatrix} W_{Ga} - W_{Ga,r} \\ W_{In} - W_{In,r} \\ W_{Sn} - W_{Sn,r} \\ W_{Zn} - W_{Zn,r} \\ W_{Al} - W_{Al,r} \end{bmatrix}$$

$$W = egin{bmatrix} U^{-1}(Ga) & 0 & 0 & 0 & 0 \ 0 & U^{-1}(In) & 0 & 0 & 0 \ 0 & 0 & U^{-1}(Sn) & 0 & 0 \ 0 & 0 & 0 & U^{-1}(Zn) & 0 \ 0 & 0 & 0 & 0 & U^{-1}(Al) \end{bmatrix}$$

W is the weight square diagonal matrix with reciprocal values of uncertainties at the fixed points. For the non-weighted version, the

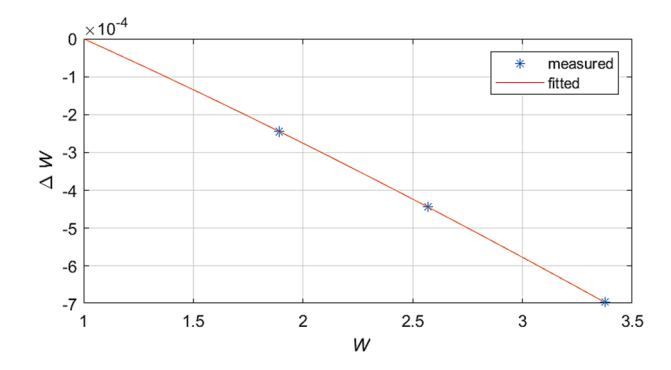


Fig. 1. Example ΔW function determined as the exact solution according to ITS-90.

V. Žužek et al. Measurement 220 (2023) 113400

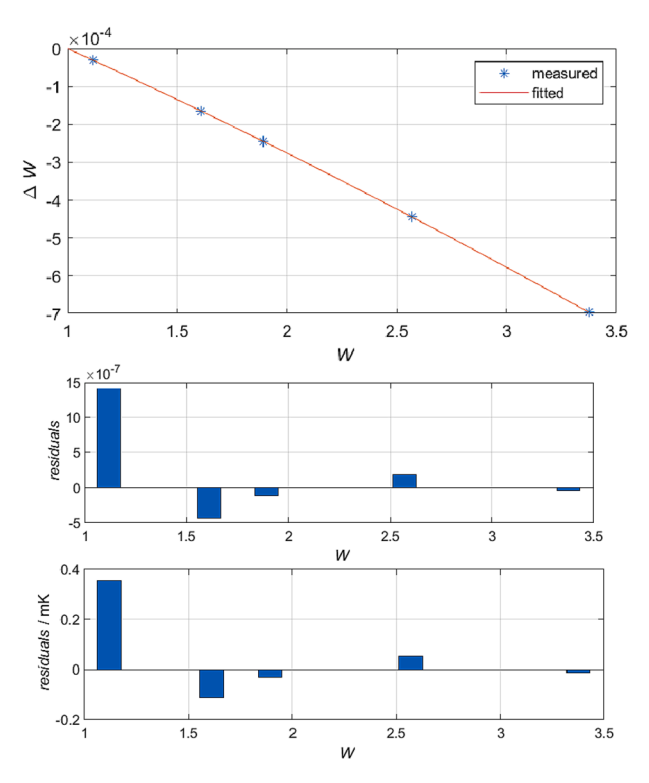


Fig. 2. Example ΔW function determined with least squares using additional gallium and indium fixed points (top). ΔW fit residuals and fit residuals in equivalent millikelvins (bottom).

elements of the main diagonal are set to 1 (which is the same as omitting the *W* matrix from equation (5).

The actual difference in interpolations for the presented example is shown in Fig. 3. The blue line is the difference between the least squares and the standard ITS-90 interpolation and the red line is the difference between the weighted least squares and ITS-90.

Once the deviation function ΔW of a SPRT at a certain subrange is known, t_{90} can be calculated for any given W in that subrange. The t_{90} calculated with different ΔW of different subranges can then be compared. The difference in calculated t_{90} between two subranges is the SRI for that particular SPRT. The pattern is the same for deviation functions in the water-zinc and water-tin subranges, except that these functions are quadratic with only two coefficients (c=0).

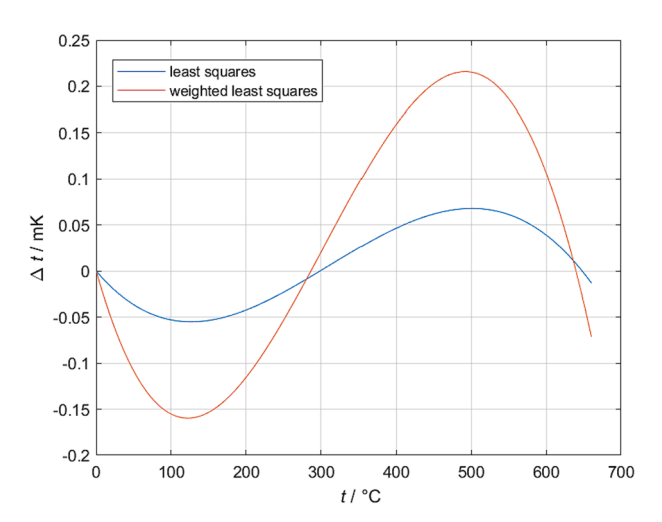


Fig. 3. Difference between interpolations in mK for the presented example.

3. Inconsistency of water-aluminum/water-zinc and water-zinc/water-tin subranges

Calibration data for a total of 30 different SPRTs was gathered from the database of Laboratory of Metrology and Quality (LMK) at the University of Ljubljana, which is the Slovenian national temperature metrology laboratory. The SPRTs were measured at all fixed points from the water-aluminum subrange and were both quartz and metal sheathed, as detailed in Table 2. Calibrated *W* values are collected in Table 3 and visually represented as *S* ratios [7] in Fig. 4.

SRI(Al:Zn) for the SPRTs from Tables 2 and 3 is presented in Fig. 5, following the ITS-90 procedure. The subranges overlap in the temperature range from the water to the zinc fixed point. The ordinate axis represents the difference in millikelvins between the calculated temperatures using the two different deviation functions. The mean SRI(Al: Zn) is shown with the thick black line and the dashed black line shows the standard deviation, relative to mean.

If we take into account also the additional fixed points of indium and gallium and calculate the coefficients of the deviation functions with the least squares method, we obtain the plot in Fig. 6. Furthermore, if the least squares are weighted, the SRI plot in Fig. 7 is obtained. The weights are reciprocal values of LMK uncertainties from Table 1. The maximum mean and standard deviation values of all three variants are collected in Table 4.

SRI(Zn:Sn) for the SPRTs from Tables 2 and 3 is shown in Fig. 8, following the ITS-90 procedure (namely, quadratic interpolations form the TPW to the freezing points of tin and zinc, or indium and tin). Here, the subranges overlap in the temperature range from the water to the tin point. Fig. 9 shows the SRI(Zn:Sn) if the indium and gallium points are included in both subranges. Fig. 10 shows the results for the weighted least squares, and again, the maximum mean and standard deviation values are in Table 4.

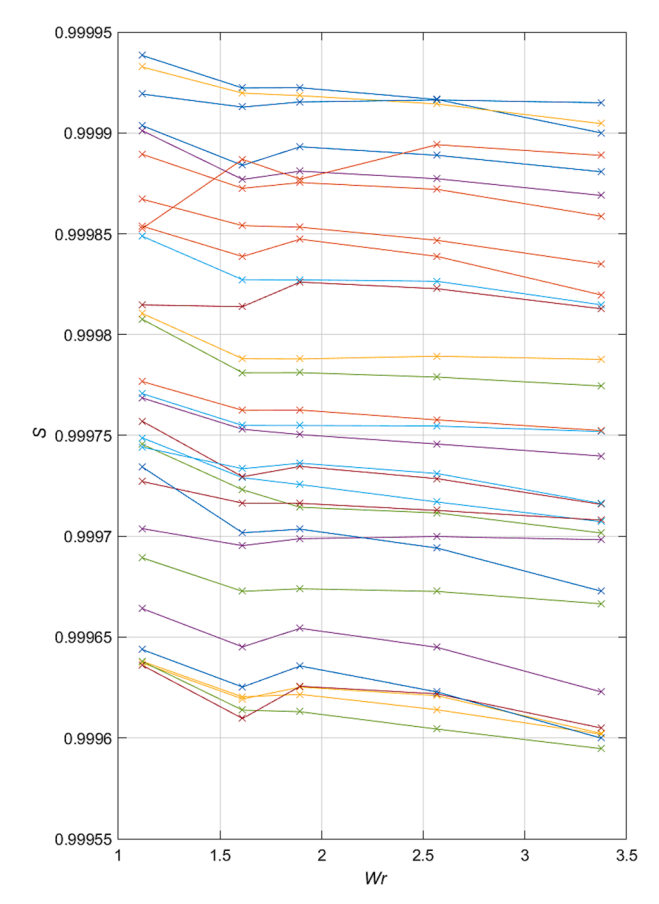


Fig. 4. S ratios of SPRTs.

Table 2 Investigated SPRTs: year of calibration, manufacturer, model, serial number and sheath type.

year of calibration	manufacturer	model designation	serial number	sheath
2020	Fluke	5699	613	metal
2020	Fluke	5681	1792	glass
2020	Fluke	5681	1698	glass
2020	AccuMac	1960	1,620,965	glass
2020	Acculvac	1880	1,880,401	metal
2020	AccuMac	1880	1,880,400	metal
2020	AccuMac	1880	1,880,003	metal
2020	AccuMac	1860	1,620,703	metal
2020	AccuMac	1860	1,620,697	metal
2020	Acculvac	1960	1,620,777	glass
2020	Fluke	5699	1,020,777	metal
2020	AccuMac	1880	1,880,084	metal
2020	Rosemount	162CE	5227	metal
2020	Rosemount	162CE 162CE	5225	metal
2020	Fluke	5684	5225 1177	
2019	Fluke	5699	495	glass metal
		162CE	495 4760	
2019 2019	Rosemount	162CE 162CE		metal
2019	Rosemount Rosemount	162CE 162CE	4789 4776	metal metal
2019	Rosemount			
		162CE 162CE	4775	metal
2019	Rosemount		5344	metal
2019	Fluke	5699	1085	metal
2018	Fluke	5684	1176	glass
2018	Fluke	5699	847	metal
2018	Fluke	5699	842	metal
2018	AccuMac	1960	1,620,775	glass
2017	AccuMac	1880	1,880,105	metal
2017	Fluke	5699	829	metal
2017	Fluke	5699	857	metal
2017	Fluke	5681	1943	glass

4. LMK fixed point uncertainties propagation

The individual uncertainties from SPRT fixed point calibrations (Table 1) propagate throughout the whole temperature subrange. They

depend on fixed point and maintenance apparatus quality and the quality of the resistance measurements. The difference in propagated uncertainties between different subranges is the main contribution to SRI.

To obtain the square of the total propagated uncertainty curve (f_T^2) , squared contributions from all used fixed points are summed, as in equation (6). The contribution from a particular fixed point is calculated as explained in [3]; specifically, two calibration curves are compared, where an error is deliberately introduced to one of them.

$$f_T^2 = f_{Ga}^{\prime 2} + f_{In}^{\prime 2} + f_{Sn}^{\prime 2} + f_{Zn}^{\prime 2} + f_{AI}^{\prime 2}$$
 (6)

Figs. 11 and 12 show the total propagated uncertainty for the water-aluminum and water-zinc subranges, following all three established calculation cases.

Furthermore, the differences in propagated uncertainty between the water-aluminum and water-zinc and between the water-zinc and water-

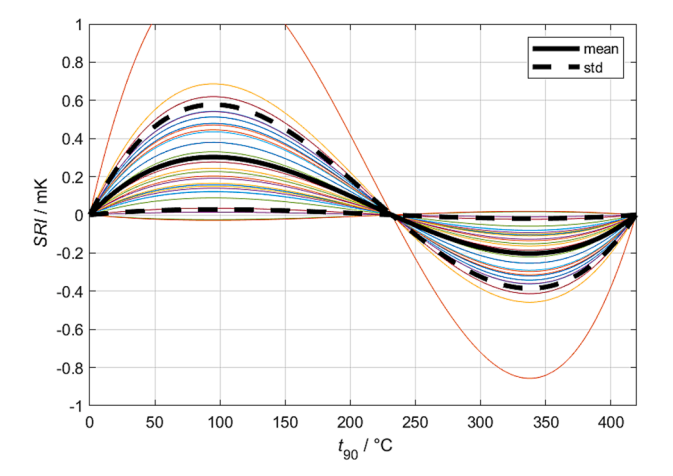


Fig. 5. ITS-90 SRI(Al:Zn).

Table 3 Investigated SPRTs: calibration values.

serial number	W_{Ga}	$W_{ m In}$	W_{Sn}	W_{Zn}	W_{Al}
613	1.11813161	1.60975447	1.89272838	2.56878637	3.37577099
1792	1.11812319	1.60971285	1.89266666	2.56867685	3.37561636
1698	1.11813093	1.60975289	1.89272490	2.56878296	3.37578188
1,620,965	1.11811155	1.60965128	1.89257488	2.56851834	3.37539031
1,880,401	1.11810883	1.60963298	1.89254265	2.56846477	3.37529968
1,880,400	1.11810921	1.60963660	1.89255274	2.56847330	3.37531289
1,880,003	1.11811018	1.60963689	1.89256075	2.56849143	3.37533329
1,620,703	1.11812750	1.60973103	1.89270224	2.56874298	3.37572517
1,620,697	1.11812161	1.60970349	1.89266137	2.56866435	3.37558012
1,620,777	1.11809612	1.60957036	1.89245989	2.56831167	3.37506255
128	1.11812720	1.60972680	1.89269145	2.56872476	3.37569731
1,880,084	1.11811615	1.60966836	1.89260230	2.56857048	3.37547286
5227	1.11812102	1.60969647	1.89264336	2.56864502	3.37556847
5225	1.11811700	1.60968833	1.89264232	2.56863920	3.37556382
1177	1.11812935	1.60974869	1.89272213	2.56878597	3.37580653
495	1.11812582	1.60972411	1.89268642	2.56871656	3.37567277
4760	1.11811650	1.60967259	1.89260832	2.56858676	3.37550417
4789	1.11810389	1.60961607	1.89252881	2.56844641	3.37529171
4776	1.11810218	1.60960227	1.89250659	2.56840370	3.37521626
4775	1.11811180	1.60965243	1.89257888	2.56853243	3.37541923
5344	1.11810665	1.60962893	1.89254443	2.56846679	3.37531478
1085	1.11810750	1.60961998	1.89253301	2.56843752	3.37523111
1176	1.11812148	1.60973287	1.89268794	2.56875123	3.37574441
847	1.11809602	1.60956974	1.89246304	2.56832262	3.37506342
842	1.11809921	1.60958548	1.89248909	2.56836020	3.37511243
1,620,775	1.11809611	1.60956637	1.89245216	2.56829668	3.37504560
1,880,105	1.11810867	1.60963935	1.89256220	2.56849541	3.37533440
829	1.11809589	1.60956382	1.89246344	2.56832400	3.37506992
857	1.11809681	1.60957333	1.89247241	2.56832551	3.37505784
1943	1.11811251	1.60965702	1.89258570	2.56853712	3.37542034

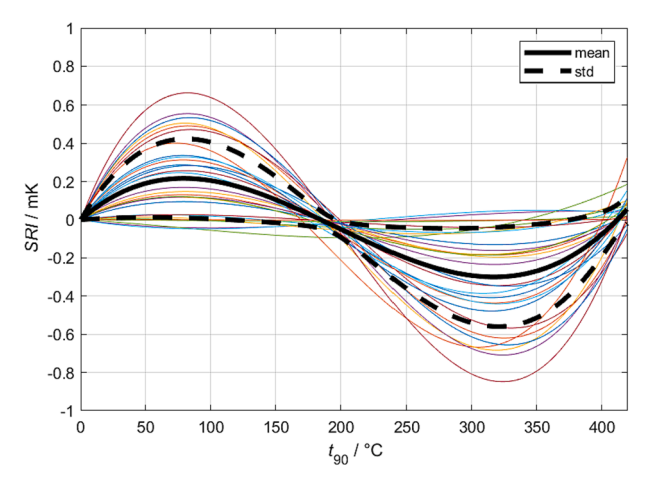


Fig. 6. SRI(Al:Zn) with indium and gallium points - least squares.

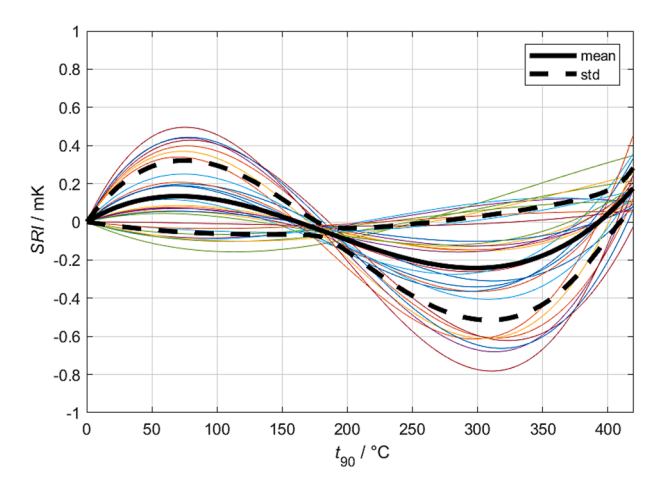


Fig. 7. SRI(Al:Zn) with weighted least squares.

Table 4 Maximum value of mean and standard deviation of SRI. The last two columns show the contribution of propagated uncertainty (PoU) to SRI and its fraction of the standard deviation, σ .

variant	SRI mean / mK	SRI σ / mK	PoU / mK	PoU/ σ
Al:Zn, ITS-90	0.30	0.27	0.24	89%
Al:Zn, least squares	0.30	0.26	0.16	62%
Al:Zn, weighted least squares	0.24	0.28	0.14	50%
Zn:Sn, ITS-90	0.71	1.25	0.75	60%
Zn:Sn, least squares	0.19	0.59	0.37	63%
Zn:Sn, weighted least squares	0.01	0.43	0.30	70%

tin subranges are shown in Figs. 13 and 14, respectively. They depend only on individual uncertainties at fixed points. For the wateraluminum/water-zinc pair of subranges, the maximum differences in propagated uncertainty are 0.24 mK for the ITS-90 case, 0.16 mK for the least squares case and 0.14 mK for the weighted least squares case. These values represent more than 50% of the calculated SRI standard deviation (last column of Table 4). The same applies for the water-zinc/water-tin pair of subranges, where differences amount to 0.75 mK for the ITS-90, 0.37 mK for the least squares and 0.30 mK for the weighted least squares case.

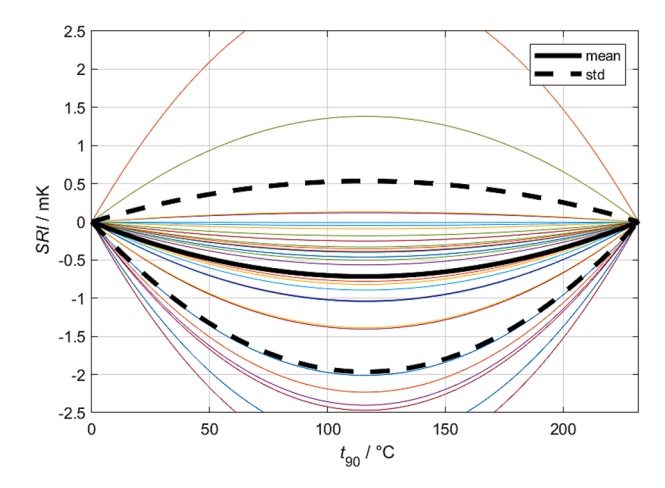


Fig. 8. ITS-90 SRI(Zn:Sn).

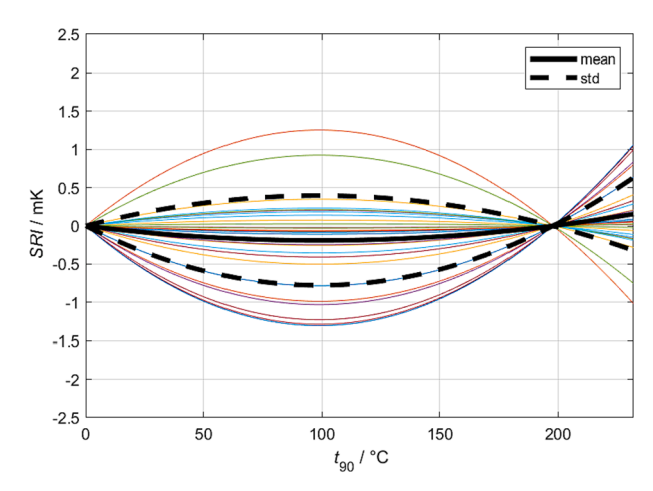


Fig. 9. SRI(Zn:Sn) with indium and gallium points – least squares.

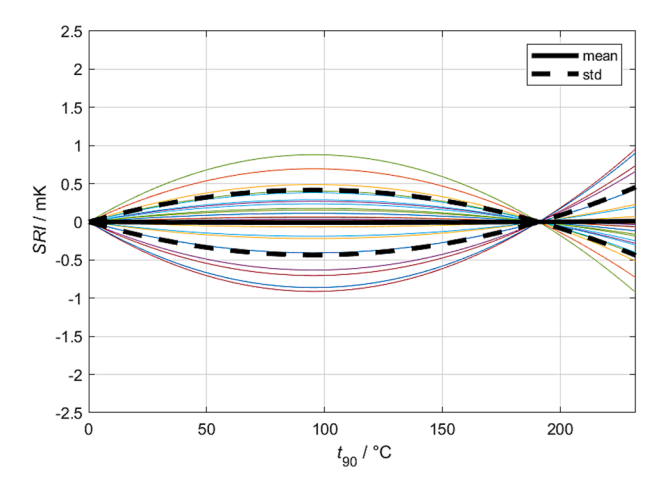


Fig. 10. SRI(Zn:Sn) with weighted least squares.

5. Conclusions

The subrange inconsistency for the water-aluminum/water-zinc and water-zinc/water-tin subrange pairs was calculated for a large ensemble of 30 SPRTs from the database of the Laboratory of metrology and quality at the University of Ljubljana. The ensemble consisted mostly of SPRTs manufactured by Fluke, Rosemount and AccuMac, both quartz and metal sheathed.

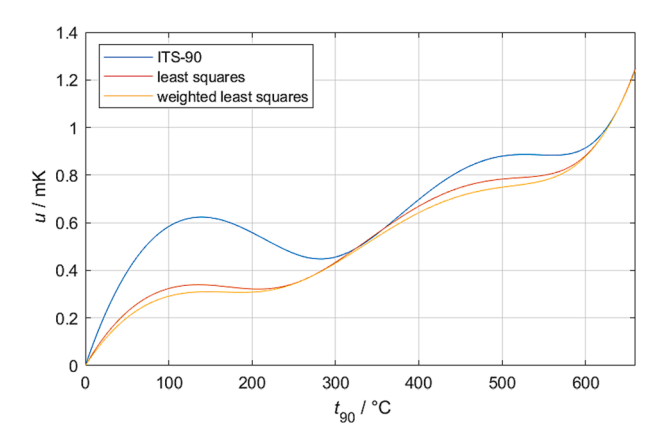


Fig. 11. Total propagated uncertainty for the water-aluminum subrange.

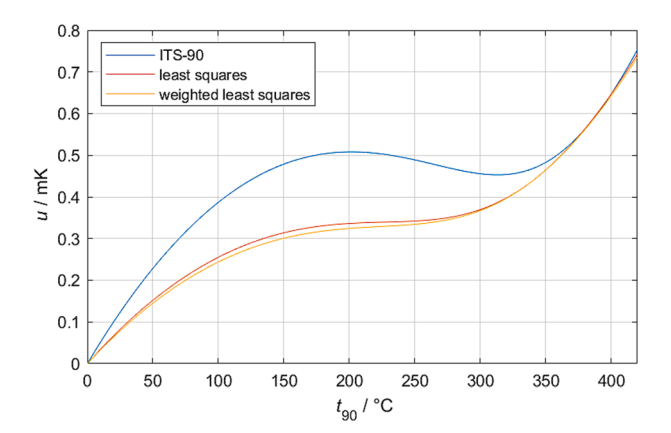


Fig. 12. Total propagated uncertainty for the water-zinc subrange.

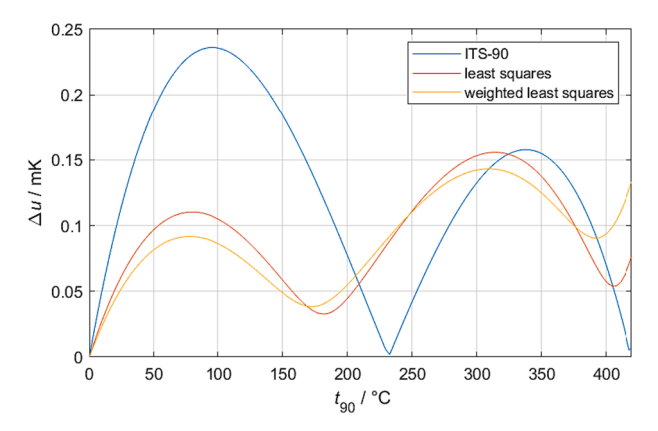


Fig. 13. Difference in propagated uncertainty between water-aluminum and water-zinc subranges – PoU contribution to SRI(Al:Zn).

Besides the ITS-90 procedure for the deviation function determination where the exact solution is used, least squares and weighted least squares approaches were also applied to the same ensemble, using redundant fixed points from the temperature subrange. In the water-aluminum/water-zinc pair of subranges, the change in subrange inconsistency mean and standard deviation values was minor. On the other hand, for the water-zinc/water-tin pair, both the mean and standard deviation values of subrange inconsistency decreased significantly with the least squares method.

The total propagated uncertainty from fixed points decreases in certain temperature ranges if the least squares methods are used, especially in the temperature range from 50 $^{\circ}$ C to 300 $^{\circ}$ C and also from

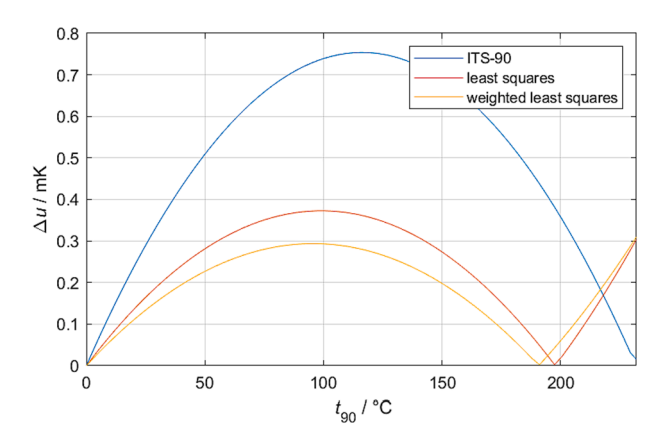


Fig. 14. Difference in propagated uncertainty between water-zinc and water-tin subranges – PoU contribution to SRI(Zn:Sn).

 $400\,^{\circ}\text{C}$ to $600\,^{\circ}\text{C}$ to lesser extent. Moreover, the difference in propagated uncertainties between different subranges also decreases significantly. Its contribution to SRI was estimated to be at least 50% in all cases.

According to the presented results, it can be advantageous to calibrate the SPRT at all available fixed points in the selected temperature subrange and then determine its deviation function with the weighted least squares method – the total propagated uncertainty from fixed points (and subrange inconsistency) are reduced in this way.

Possible steps for further investigation of subrange inconsistency reduction are to include more SPRTs from different manufacturers and to include more temperature subrange pairs.

Disclaimer

The article reflects only the authors' view and EURAMET is not responsible for any use that may be made of the information it contains.

Funding

This paper has been written through funding received from the EU EMPIR program co-financed by the Participating States and from the European Union's Horizon 2020 research and innovation program, specifically from the EMPIR project 18SIB02 "Realizing the redefined kelvin".

It was also partially supported by the Ministry of Economic Development and Technology, Metrology Institute of Republic Slovenia, in scope of contract 6401-18/2008/70 for the national standard laboratory for the field of thermodynamic temperature and humidity and by the ARRS project J2-1721 "New generation of industrial noise thermometers (Nova generacija industrijskih šumnih termometrov)".

CRediT authorship contribution statement

Vincencij Žužek: Conceptualization, Methodology, Software, Formal analysis, Investigation, Resources, Data curation, Writing – original draft, Visualization. Richard Rusby: Validation, Writing – review & editing, Supervision. Jonathan Pearce: Writing – review & editing. Andrea Peruzzi: Writing – review & editing. Jovan Bojkovski: Conceptualization, Methodology, Resources, Writing – review & editing, Supervision, Project administration, Funding acquisition.

Declaration of Competing Interest

The authors declare that they have no known competing financial interests or personal relationships that could have appeared to influence the work reported in this paper.

Data availability

Data will be made available on request.

References

- H. Preston-Thomas, The International Temperature Scale of 1990 (ITS-90), Metrologia 27 (1) (Jan. 1990) 3–10, https://doi.org/10.1088/0026-1394/27/1/002
- [2] Bureau International des Poids et Mesures, The International System of Units (SI), 9th ed., 2019.
- [3] Consultative Committee for Thermometry, Guide to the Realization of the ITS-90: Chapter 5: Platinum resistance thermometry, 2021.
- [4] A. Peruzzi, R.L. Rusby, J.V. Pearce, L. Eusebio, J. Bojkovski, V. Žužek, Survey of subrange inconsistency of long-stem standard platinum resistance thermometers, Metrologia 58 (3) (Jun. 2021), 035009, https://doi.org/10.1088/1681-7575/ shege1
- [5] D.R. White, P.M.C. Rourke, Standard platinum resistance thermometer interpolations in a revised temperature scale, Metrologia 57 (3) (Jun. 2020), 035003, https://doi.org/10.1088/1681-7575/ab6b3c.
- [6] R.L. Rusby, J.V. Pearce, C.J. Elliott, Considerations Relating to Type 1 and Type 3 Non-uniqueness in SPRT Interpolations of the ITS-90, Int. J. Thermophys. 38 (12) (Dec. 2017) 186, https://doi.org/10.1007/s10765-017-2319-2.

- [7] D.R. White, G.F. Strouse, Observations on sub-range inconsistency in the SPRT interpolations of ITS-90, Metrologia 46 (1) (Feb. 2009) 101–108, https://doi.org/10.1088/0026-1394/46/1/013.
- [8] K. Zhiru, L. Jingbo, L. Xiaoting, Study of the ITS-90 non-uniqueness for the standard platinum resistance thermometer in the sub-range 0 C to 419.527 C, Metrologia 39 (2) (Apr. 2002) 127–133, https://doi.org/10.1088/0026-1394/39/ 2/2.
- [9] G. Machin, M. Sadli, J. Pearce, J. Engert, R.M. Gavioso, Towards realising the redefined kelvin, Measurement 201 (Sep. 2022), 111725, https://doi.org/ 10.1016/j.measurement.2022.111725.
- [10] D.R. White, The propagation of uncertainty with non-Lagrangian interpolation, Metrologia 38 (1) (Feb. 2001) 63–69, https://doi.org/10.1088/0026-1394/38/1/
- [11] P.M.C. Rourke, ITS-90 reproducibility, xenon fixed point substitution and new interpolating equations between 13.8033 K and 273.16 K, Metrologia 58 (5) (2021) 055004, https://doi.org/10.1088/1681-7575/abfd8e.
- [12] P.P.M. Steur, F. Pavese, The ITS-90: A review of the evolution of the cryogenic ranges since 1990 and a view of its future after the new kelvin definition, Measurement 159 (Jul. 2020), 107792, https://doi.org/10.1016/j. measurement.2020.107792.
- [13] J.P. Sun, T. Li, X.P. Hao, J. Pan, J.X. Zeng, New interpolating equations of ITS-90 for SPRTs and HTSPRTs for the temperature range 419.527 ° C-961.78 ° C, Metrologia 57 (4) (2020) 045001, https://doi.org/10.1088/1681-7575/ab8828.